RSC Advances




ROYAL SOCIETY OF CHEMISTRY

www.rsc.org/advances

Cite this: DOI: 10.1039/c0xx00000x

www.rsc.org/xxxxxx

ARTICLE TYPE

# DNA-modified graphene quantum dots as a sensing platform for detection of $Hg^{2+}$ in living cells

**Xin Zhao,[a] Jinsuo Gao,[a] Xin He,[a] Longchao Cong,[a] Huimin Zhao,[a] Xiaoyu Li,[b] Feng Tan*[,a]**

***Received (in XXX, XXX) Xth XXXXXXXXX 20XX, Accepted Xth XXXXXXXXX 20XX***

**DOI: 10.1039/b000000x**

**Detection of metal ions in living cells is significant in environmental monitoring and health risk assessment. This paper reported a simple and facile method for the detection of $Hg^{2+}$ ions in Hela cells through fluorescence image, which was based on the fluorescence quenching in thymine-rich DNA modified graphene quantum dots (DNA-GQDs) in the presence of $Hg^{2+}$. The decrease in the fluorescence intensity was attributed to the electron transfer of DNA-GQDs due to $Hg^{2+}$ bound to thymine bases of the DNA, resulting in a T-T mismatch hairpin structure. The method shows high selectivity and sensitivity. This present sensing platform will have broad applications in biological imaging and environmental monitoring.**

Mercury is a widespread pollutant and produces serious effects on both eco-environment and human health.[1] Divalent mercuric ion ($Hg^{2+}$) is one of the most prevalent forms of mercury contamination and can transform more poisonous methylmercury by microbial biomethylation.[2] They can accumulate in human body through food chain and affect nervous, immune, and digestive systems and cause damages of kidney, liver, and brain.[3] Therefore, facile monitoring of $Hg^{2+}$ is very important in the fields of environmental monitoring, food safety, and toxicity assessment. To date, several methods for the detection of $Hg^{2+}$ ions have been developed such as electrochemical,[4] fluorescent,[5] atomic absorption/emission spectral,[6] and colorimetric assays.[7] Among these methods, the method based on fluorescence probes provides great advantages including ease of operation, rapid response, and especial capacity of real-time and in situ monitoring of the dynamic biological processes in living organism and cells.

Graphene quantum dots (GQDs) are graphene sheets, with size less than 100 nm and unique $sp^2$ and $sp^3$ hybrid structure. Besides the unique electronic, optical, thermal, mechanical, and chemical properties of graphene, GQDs show outstanding luminescent performance due to efficient quantum confinement and edge effects.[8] Compared with the conventional dye molecules and semiconductor quantum dots (QDs), GQDs have many specific advantages such as low toxicity, high water solubility, excellent biocompatibility, and stable photoluminescence.[9] Due to these merits, GQDs are expected to be excellent alternative to organic dyes and semiconductor QDs for fluorescence sensing platforms and bioimaging.[10] Various GQDs-based fluorescence probes have been reported for the detection of metal ions,[11] small organic molecules,[12] toxins,[13] pH,[14] and biomolecules.[15] Recently, several simple $Hg^{2+}$ sensors were developed based on quenching of fluorescence *via* electron transfer in presence of $Hg^{2+}$ showing advantages of GQDs as a efficient fluorescence probe.[16] However, there researches are focus on *in vitro* analysis while *in vivo* assays are rarely reported.[17]

Herein, we report a simple and facile method for selective detection of $Hg^{2+}$ in living cells based on single-stranded thymine-rich DNA functionalized GQDs (DNA-GQDs). Scheme 1 shows the principle for the detection of $Hg^{2+}$ with DNA-GQDs. In the presence of $Hg^{2+}$, thymine-rich DNAs form a rigid hairpin structure due to the strong coordination of the spatially separated thymine bases for $Hg^{2+}$, resulting in the decrease in the fluorescence emission of DNA-GQDs. The response is fast and insensitive to solution pH and ionic strength. The sensor shows high selectivity for $Hg^{2+}$ over other metal ions and allows the detection of $Hg^{2+}$ in living cells. To the best of our knowledge, this is the first report based on GQDs for the detection of metal ions in living cells.

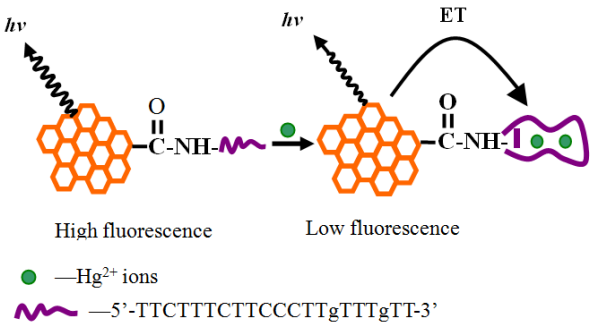


**Sch. 1** Schematic diagram of DNA-GQDs for the detection of $Hg^{2+}$

GQDs were initially synthesized by a hydrothermal approach according to the previous method with minor modifications.[18] The as-prepared GQDs was characterized by AFM and TEM, as shown in Fig. 1. AFM shows good dispersion with a single layer thickness (~0.8 nm) and diameter of ~20 nm. GQDs with similar size can be clearly observed though there are some aggregation during TEM analysis due to without enough ultrasonication dispersion.

The GQDs had a broaden absorption band centered at 340 nm and exhibited strong fluorescent emission peaks from 370 nm to 420 nm depending on the excitation wavelengths (Fig.S1 and S2

in ESI†). The strongest emission peak at 420 nm was achieved under 320 nm UV excitation. To functionalize GQDs, the single-stranded DNA (5'-$NH_2$C6-TTCTTTCTTCCCTTGTTTGTT-3') were immobilized on GQDs by the amino group reaction. We measured the zeta potential value of GQDs before and after DNA modification, and found the value changed to -9.01 mV from -2.37 mV after the modification. The negative shift was attributed to the negative charges of DNAs.

FTIR spectra of GODs before and after the DNA modification were given (Fig.S3 in ESI†). The broad intense bands at ~3450 $cm^{-1}$ and ~3350 $cm^{-1}$ were assigned to O–H stretching vibrations of the C–OH groups and N–H stretching vibrations of the C–NH groups, respectively. The peaks at 1640 $cm^{-1}$ and 1255 $cm^{-1}$ were attributed to C=O and C-O stretching vibrations from the carboxylic group, respectively. The peak at 1400 $cm^{-1}$ was attributed to skeletal vibration from graphene domain,[19]. The peak at 1130 $cm^{-1}$ was attributed to C-O-C asymmetry stretching vibrations from 2-deoxyribose. The next peaks 1130 $cm^{-1}$ and 990 $cm^{-1}$ were assigned to P=O and P-O $cm^{-1}$ stretching vibrations from phosphoric group.

In additional, the emission peak of DNA-GQDs was red-shifted to 460 nm and its peak intensity increased ~50% relative to that of GQDs, as shown in Fig. 2. All these results above indicated that DNA was successfully attached onto GODs by the modification reaction.

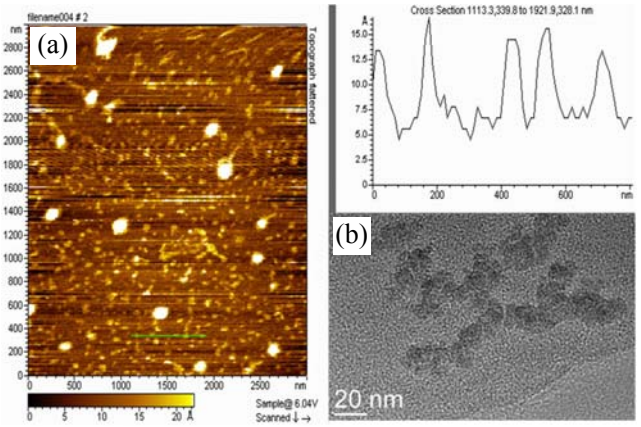


Fig. 1 AFM (a) and TEM (b) of the prepared GODs

Fig. 2 also shows the fluorescence emission spectra of DNA-GQDs before and after the addition of 10 μM $Hg^{2+}$. The emission peak intensity decreased ~90% of the initial peak intensity of DNA-GQDs after the addition. The decrease in its fluorescence intensity was attributed to the electron transfer quenching of DNA-GQDs by $Hg^{2+}$ bound to the thymine bases of DNAs to form a nonradiative T-T mismatch hairpin structure.[20] However, when GQDs without DNAs modification was added the same concentration $Hg^{2+}$, there was only a slight decrease in the fluorescence intensity of the GQDs. This change might be attributed to the coordination of carboxyl groups on the surface of GQDs for $Hg^{2+}$.

The quenching dynamics of DNA-GQDs by $Hg^{2+}$ was studied. The fluorescence signal of DNA-GQDs rapidly decreased upon the addition of $Hg^{2+}$ and reached a steady-state value of ~90% quenching of the initial fluorescence of DNA-GQDs after 1 min (Fig.S3 in ESI†). It was known that GQDs is highly sensitive to pH and ionic strength due to the presence of carboxyl groups on their surfaces.[21] However, the prepared DNA-GQDs indicated strong and relative stable fluorescence emission in the physiological pH range from 6.0 to 8.0 (Fig.S4 in ESI†). Effect of pH on the quenching efficiency was studied. Results showed that there was no any influence on the quenching in the pH range. Addition of salt (NaCl) with concentrations from 0.05 M to 0.5 M did not produce any effect in the fluorescence quenching of DNA-GQDs in the presence of $Hg^{2+}$. These characteristics provide significant advantages for the detection $Hg^{2+}$ in living cells.

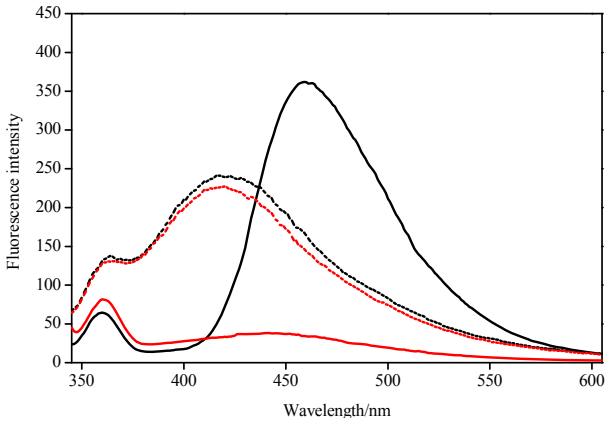


**Fig. 2** Fluorescence emission spectra of DNA-GQDs (solid) and GQDs without DNAs modification (dash) before (black) and after (red) the addition of 10 μM $Hg^{2+}$ in 10 mM PBS buffer (pH 7.4). The excitation wavelength was 320 nm.

Fig.3 shows the fluorescence emission spectra of DNA-GQDs in the presence of different concentrations $Hg^{2+}$. The fluorescence intensity of DNA-GQDs at 460 nm decreased gradually as the concentrations of $Hg^{2+}$ increased. ~90% of the initial fluorescence was quenched at the addition of 10 μM $Hg^{2+}$. Further the increase of the $Hg^{2+}$ concentrations couldn't completely quench the fluorescence of DNA-GQDs. A linear calibration curve between $F/F_0$ of DNA-GQDs and the concentrations of $Hg^{2+}$ from 1 nM to 10 μM was achieved, with a linear correlation coefficient ($R^2$) of 0.9974. The limit of detection was estimated to be 0.25 nM based on 3 $S_D/k$, where $S_D$ is the standard deviation of the blank signal of DNA-GQDs and $k$ is the slope of the calibration curve. A detailed comparison between the present method with similar methods was given (Table.S1 in ESI†). LOD achieved by the presence method is lower than that of most previous results, and importantly, our method provides better selectivity due to modification of GQDs with thymine-rich DNAs.

In order to investigate the selectivity of the method for $Hg^{2+}$, we examined the fluorescence emission spectra of DNA-GQDs in the presence of different individual metal ions including $Na^+$, $K^+$, $Li^+$, $Ag^+$, $Pb^{2+}$, $Mg^{2+}$, $Ni^{2+}$, $Zn^{2+}$, $Co^{2+}$, $Cd^{2+}$, $Cu^{2+}$, $Mn^{2+}$, $Ca^{2+}$ and $Fe^{3+}$ at a concentration of 50 μM, which is 5 times that of $Hg^{2+}$ resulting in 90% quenching of the initial fluorescence of DNA-GQDs. Results showed that $F/F_0$ of DNA-GQDs was nearly not changed in the presence of these metal ions at this level, as shown in Fig. 4. In addition, DNA-GQDs also were highly robust towards various anions such as $Cl^{1-}$, $NO^{3-}$, $SO_4^{2-}$, and $PO_4^{3-}$. This fact indicated that the present sensor had a high selectivity and specificity for $Hg^{2+}$ against other ions. Such an

excellent specificity was attributed to the strong affinity binding of the T-T mismatch bases of DNAs for $Hg^{2+}$.

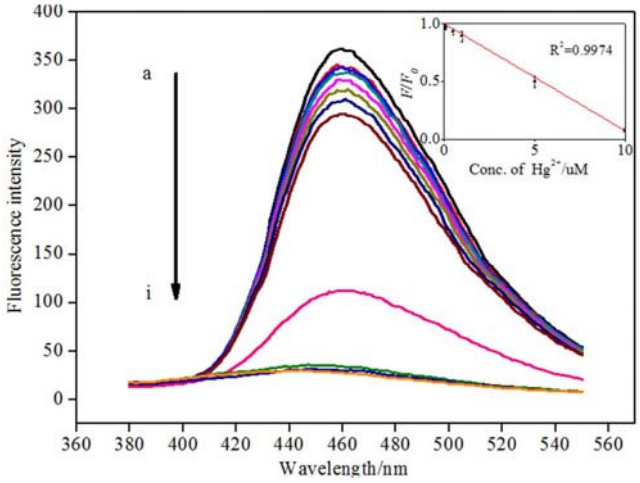


**Fig.3** Fluorescence emission spectra of DNA-GQDs in the presence of $Hg^{2+}$ at different concentrations (from a to i: 0, 0.001, 0.005, 0.01, 0.05, 0.1, 0.5, 1, 5, 10, 20, 30 μM). The insert shows a calibration curve of $F/F_0$ of DNA-GQDs *versus* $Hg^{2+}$concentrations (μM). $F_0$ and $F$ are the fluorescence emission intensities of DNA-GQDs at 460 nm in the absence and presence of $Hg^{2+}$.

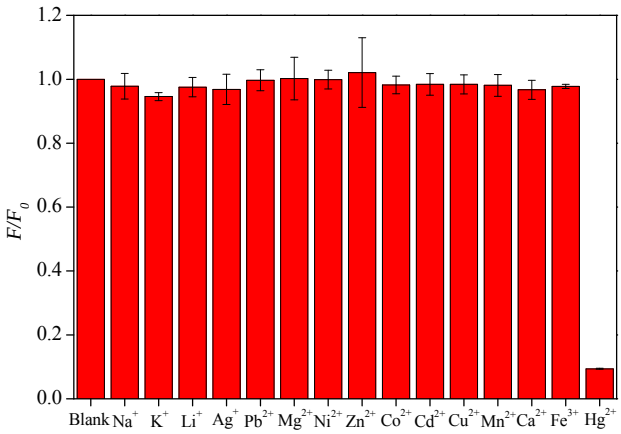


**Fig. 4** The fluorescence intensity ratio ($F/F_0$) of DNA-GQDs at 460 nm in the presence and absence of various individual metal ions (50 μM) and $Hg^{2+}$ (10 μM), respectively.

A further study has been carried out to demonstrate the availability of the sensor for the detection $Hg^{2+}$ in biological samples. Hela cells (human cervical cancer cells) were plated on glass coverslips and allowed to adhere for 24 h in H-DMEM supplemented with 10% fetal bovine serum at 37 $^{o}$C. The cells were incubated with DNA-GQDs for half an hour, followed by washing three times with PBS buffer to remove the remaining DNA-GQDs. After that, the cells were incubated with $Hg^{2+}$ (0 μM, 1 μM, 10 μM, and 20 μM) for another half an hour, respectively, and then washed with PBS buffer. Fig. 5 shows the bright field, fluorescence, and overlay images of Hela cells with DNA-GQDs in the presence of $Hg^{2+}$ using laser confocal microscope. The overlay of fluorescence and bright field images indicated that the fluorescence signals were localized in the intracellular area, indicating that DNA-GQDs were cell membrane permeable. With the increase of $Hg^{2+}$ concentrations, the fluorescence signal weakened gradually and completely disappeared at 20 μM $Hg^{2+}$. This fact indicated the ability of DNA-GQDs probe for the detection of $Hg^{2+}$ in living cells.

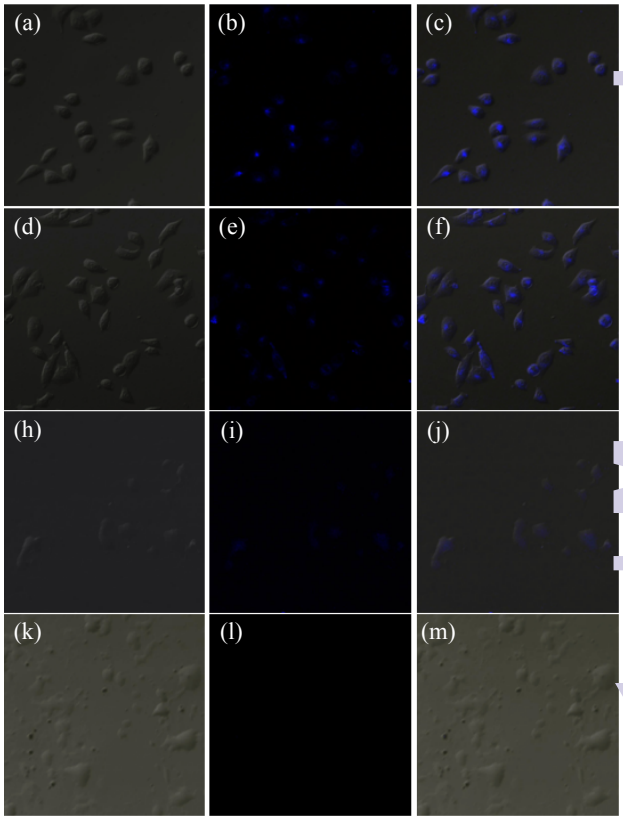


**Fig. 5** Bright field (a, d, h, and k), fluorescence (b, e, I, and l), and overlay (c, f, j, and m) images of the Hela cells with DNA-GQDs after adding 0 μM (a, b, and c), 1 μM (d, e, and f), 10 μM (h, I, and j), 20 μM (k, l, and m) $Hg^{2+}$ using scanning confocal microscope.

Biocompatibility need to be considered for applications in living cells. Previous results showed different biocompatibility for graphene material depending on its' physical-chemical properties,[22] which is related to the preparation methods. Here the DNA-GODs-induced cytotoxic effects on Hela cells were evaluated by MTT assay, as shown in Fig. 6. The cells viability had no change after exposure to 50 μg/mL DNA-GODs for 24 h at 37 $^{o}$C, showing excellent biocompatibility. The viability decreased to ~75% when the concentration of DNA-GODs increased 250 μg/mL. This indicated there was small toxic effect at high concentration. Since the cells showed fast uptake of DNA-GODs and the exposure time of DNA-GODs for the detection of $Hg^{2+}$ in Hela cells was less than one hour, the resulting effect was small and negligible.

In summary, we have demonstrated a simple and facile method based on DNA-GQDs fluorescence probe for the detection of $Hg^{2+}$ in living cells. The sensing mechanism was base on the strong coordination of T-T mismatch bases for $Hg^{2+}$ resulting in quenching in the fluorescence of DNA-GQDs. The sensor showed high selectivity and could detect $Hg^{2+}$ at concentrations as low as 0.25 nM in aqueous solution. Because of its good water solubility and low cytotoxicity, the sensor achieve rapid and facile detection of $Hg^{2+}$ in Hela cells. We expect this sensing platform will have broad applications in biologic

imaging and environmental monitoring.

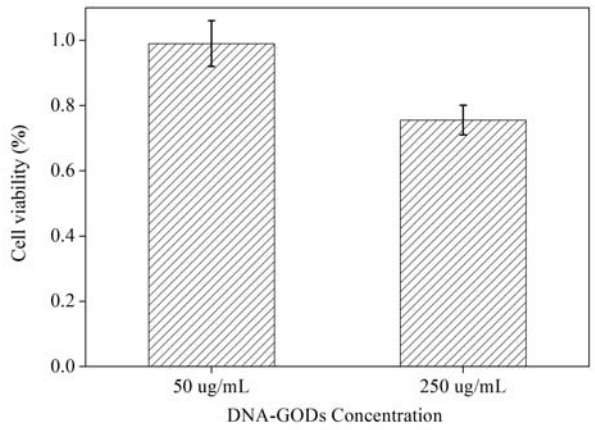


**Fig. 6** Effects of DNA-GODs at various concentrations on the viability of Hela cells quantified by MTT assay.

## Notes and references

[a] *Key Laboratory of Industrial Ecology and Environmental Engineering (MOE), School of Environmental Science and Technology,Dalian University of Technology, Dalian 116024, China. Fax: 86-411-84707965; Tel: 86-411-84707965; E-mail: tanf@dlut.edu.cn*

[b] *School of Life Science and Biotechnology, Dalian University of Technology, Dalian 116024, China.*

† Electronic Supplementary Information (ESI) available: Experimental details, characterization of GQDs, and other information. See DOI: 10.1039/b000000x/

1 (a) C.T. Driscoll, R.P. Mason, H.M. Chan, D.J. Jacob, N. Pirrone, *Environ, Sci. Technol.,* 2013, 47, 4967; (b) H. Gibb, K.G. O'Leary, *Environ. Health. Perspect.,* 2014, 122, 667.

2 C.C. Gilmour, M. Podar, A.L. Bullock, A.M. Graham, S.D. Brown, A.C. Somenahally, A. Johns, R.A. Hurt, K.L. Bailey, D.A. Elias, *Environ. Sci. Technol.,* 2013, 47, 11810.

3 A. Bhan, N.N. Sarkar, *Rev. Environ. Health*, 2005, 20, 39.

4 (a) S.J. He, D. LI, C.F. Zhu, S.P. Song, L.H. Wang, Y.T. Long, C.H. Fan, *Chem. Commun.*, 2008, 40. 4885. (b) H. Park, S.J. Hwang, K. Kim, *Electrochem. Commun.,* 2012, 24, 100; (c) Z.Z. Lin, X.H. Li, H.B. Kraatz, *Anal. Chem.,* 2011, 83, 6896.

5 (a) B.C. Ye, B.C. Yin, *Angew. Chem. Int. Ed.,* 2008, 47, 8386; (b) X.L. Zhang, Y. Xiao, X.H. Qian, *Angew. Chem. Int. Ed.,* 2008, 47, 8025; (c) J.P. Xie, Y.G. Zheng, J.Y. Ying, *Chem. Commun.,* 2010, 46, 961.

6 (a) S. Gil, I. Lavilla, C. Bendicho, *Anal. Chem.*, 2006, 78, 6260; (b) B. Jackson, V. Taylor, R.A. Baker, E. Miller, *Environ. Sci. Technol.,* 2009, 43, 2463.

7 (a) J.S. Lee, M.S. Han, C.A. Mirkin, *Angew. Chem. Int. Ed.,* 2007, 46, 4093; (b) S.J. He, C.F. Zhu, S.P. Song, L.H. Wang, Y.T Long, C.H. Fan, *Chem. Commun.*, 2008, 40, 4885; (c) C.W. Liu, Y.T. Hsieh, C.C. Huang, Z. H. Lin, H.T. Chang, *Chem. Commun.*, 2008, 40, 2242; (d) Y.J. Kim, R.C. Johnson, J.T. Hupp, *Nano lett.*, 2001, 1, 165; (e) G.K. Darbha, A.K. Singh, U.S. Rai, E. Yu, H.T. Yu, P.C. Ray, *J. Am. Chem. Soc*., 2008, 130, 8038.

8 (a) R. Sekiya, Y. Uemura, H. Murakami, T. Haino, *Angew. Chem. Int. Ed.,* 2014, 53, 5619; (b) L. A. Ponomarenko, F. Schedin, M. I. Katsnelson, R. Yang, E. W. Hill, K. S. Novoselov and A. K. Geim, *Science*, 2008, **320**, 356.

9 (b) D.Y. Pan, J.C. Zhang, Z. Li, M.H. Wu, *Adv. Mater.*, 2010, 22, 734; (b) S.H. Jin, D.H. Kim, G.H. Jun, S.H. Hong, S. Jeon, *ACS Nano*, 2013, 7, 1239.

10 J.H. Shen, Y.H. Zhu, X.L. Yang and C.Z. Li, *Chem. Commun.*, 2012, 48, 3868-3699; (b) Z.T. Fan, Y.C. Li, X.H. Li, L.Z. Fan, S.X. Zhou, D.C. Fang, S.H. Yang, *Carbon*, 2014, 70, 149; (c) V. Kumar, V. Singh, S. Umrao, V. Parashar, S. Abraham, A.K. Singh, G. Nath, P.S. Saxena, A. Srivastava, *Biosens. Bioelectron.,* 2014, 4, 21101.

11 (a) M. Li, X.J. Zhou, S.W. Guo, N.Q. Wu, *Biosens. Bioelectron.,* 2013, 43, 69; (b) Y.X. Qi, M. Zhang, Q.Q. Fu, R. Liu, G.Y. Yue, *Chem. Commun*., 2013, 49, 10599; (c) S.H. Li, Y.C. Li, J. Cao, J. Zhu, L.Z. Fan, *Anal. Chem*., 2014, 86, 10201; (d) X. Ran, H.J. Sun, F. Pu, J.S. Ren, X.G. Qu, *Chem. Commun.,* 2013, 49, 1079.

12. (a) S. Chen, X. Hai, X.W. Chen, J.H. Wang, *Anal. Chem.*, 2014, 86, 6689; (b) D. Dutta, S. Chandra, A.K. Swain, D. Bahadur, *Anal. Chem.*, 2014, 86, 5914; (c) Y. Zhou, Z.B. Qu, Y.B. Zeng, T.S. Zhou, G.Y. Shi, *Biosens. Bioelectron.*,2014, 52, 317.

13 J.P. Tian, H.M. Zhao, Y.B. Zhang, H.T. Yu, S. Chen, *Sens. Actuators, B*, 2014, 196, 532.

14 K. Paek, H. Yang, J. Lee, J. Park, B.J. Kim, *ACS Nano*, 2014, 8, 2848.

15 (a) J.J. Lu, M. Yan, L. Ge, S.G. Ge, S.W. Wang, J.X. Yan, J.H. Yu, *Biosens. Bioelectron.*,2013, 47, 271; (b) I. Al-Ogaidi, H.L. Gou, Z.P. Aguilar, S.W. Guo, A.K. Melconian, A.K.A. Al-Kazaz, F.K. Meng, N.Q. Wu, *Chem. Commun*., 2014, 50, 1344; (c) Z.S. Qian, X.Y. Shan, L.J. Chai, J.J. MA, J.R. Chen, H. Feng, Nanoscale, 2014, 6, 5671; (d) Z.S. Qian, X.Y. Shan, L.J. Chai, J.J. Ma, J.R. Chen, H. Feng, *Chem. Eur. J.,* 2014, 20, 16065.

16 (a) Z.S. Qian, X.Y. Shan, L.J. Chai, J.R. Chen, H. Feng, *Biosens. Bioelectron.,2015, 68, 225-231;* (b) R.Z. Zhang, W. Chen, *Biosens. Bioelectron.,* 2014, 55, 83-90*;* (c) X. Cui, L. Zhu, J. Wu, Y. Hou, P.Y. Wang, Z.n. Wang, M. Yang, *Biosens. Bioelectron.*, 2015, 63, 506-512.

17 (a) D.Y. Pan, J.C. Zhang, Z. Li, M.H. Wu, Adv. Mater., 2010, 22, 734-738; (b) P.J Luo, Y. Qiu, X,F. Guan, L,Q, Jiang, Phys. Chem. Chem. Phys., 2014, 16, 19011, 19016.

18 (a) Z. S. Qian, X. Y. Shan, L. J. Chai, J. J. Ma, J. R. Chen and H. Feng, *Biosens. Bioelectron.,* 2014, **60**, 64; (b) Y. Dong, J. Shao, C. Chen, H. Li, R. Wang, Y. Chi, X. Lin and G. Chen, *Carbon*, 2012, **50**, 4738; (c) D. Pan, J. C. Zhang, Z. Li and M. H. Wu, *Adv. Mater.*, 2010, **22**, 734.

19 V. Štengl, S. Bakardjieva, J. Henych, K. Lang, M. Kormunda, Carbon, 2013, 63, 537.

20 J. S. Lee, M. S. Han and Chad A. Mirkin, *Angew. Chem. Int. Ed.*, 2007, **46**, 4093.

21 (a) Y. Z. He, X. X. Wang, J. Sun, S. F. Jiao, H. Q. Chen, F. Gao, L. Wang, *Anal. Chim. Acta*, 2014, **810**, 71; (b) J. Shen, Y. Zhu, X. Yang and C. Li, *Chem. Commun.*, 2012, **48**, 3686; J.L. Chen, X.P. Yan, *Chem. Commun.,* 2011, 47, 3135 .

22 A. M. Pinto, I. C. Goncalves, F. D. Magalhães, *Colloids Surf., B*, 2013, 111, 188.